Proceedings of the 38th
Conference on Decision & Control
Phoenix, Arizona USA • December 1999

Simple Motion Planning Strategies for Spherobot: A Spherical Mobile Robot

Ranjan Mukherjee, Mark A. Minor, Jay T. Pukrushpan
Department of Mechanical Engineering
Michigan State University
East Lansing, MI 48824-1226
email: mukherji@egr.msu.edu

Abstract

Mobile robots have been traditionally designed with wheels and few have explored designs with spherical exo-skeletons. A spherical mobile robot that offers to have a number of advantages, is proposed in this paper. The success of our design is contingent upon development of control strategies for reconfiguration of the sphere. In this paper we address the open-loop control problem and present two strategies for reconfiguration. The first strategy uses spherical triangles to bring the sphere to a desired position with a desired orientation. The second strategy uses a specific kinematic model and generates a trajectory comprised of straight lines and circular arc segments. As compared to exisiting motion planners, our strategies require less computation and provide scope for easy implementation.

1 Introduction

Mobile robots, for most applications have been designed with wheels, possibly due to our kinship with automobiles. Enhanced mobility and stability have been typically achieved using multiple wheels, large wheels, multi-wheel drives, broad wheel bases, traction enhancing devices, articulated body configurations, etc. All these designs have relied on traditional use of the wheel as a quasi-static device. A dynamically stabilized single-wheel robot was developed only recently by Brown and Xu [3].

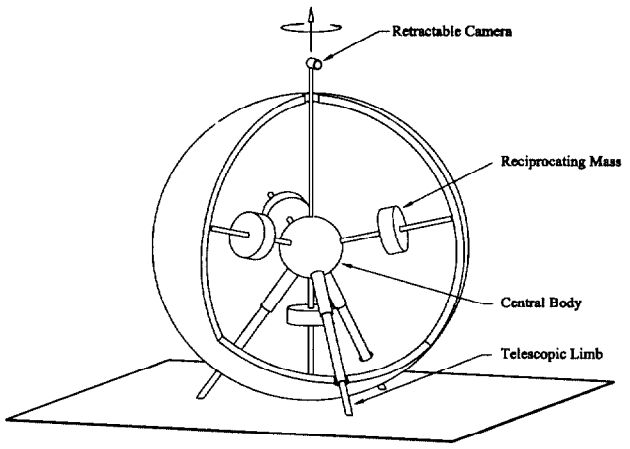

Figure 1. The Spherobot

Similar to Gyrover, which differs from traditional quasi-static designs, a few designs have been proposed for spherical robots with internal mechanisms for propulsion. An omnidirectional steering robot comprising of a spherical wheel, an arch-shaped body, and an arm-like internal mechanism, was proposed by Koshiyama and Yamafuji [7]. This design allows a limited range of lateral roll and fails to exploit the maneuverability available with spherical exo-skeletons. The first true spherical robot was developed by Halme, et.al. [4]. This robot uses a single-wheeled device constrained within the spherical cavity that generates motion by creating unbalance and changes heading by turning the wheel axis. A similar design, where the drive wheel was replaced by a car, was later proposed by Bicchi, et.al. [2]. Both robot designs [2], [4] complicate the control problem by imposing nonholonomic constraints both inside and outside the sphere.

We are engaged in research and development of Spherobot, a mobile robot with a spherical exo-skeleton and a novel internal propulsion mechanism. The propulsion mechanism will distribute weights radially along spokes fixed inside the sphere and enable the robot to accelerate, move with constant velocity, or servo at a point. For mission capabilities, we propose to incorporate a retractable camera and telescopic limbs, as shown in Fig.1. The limbs and the camera will be deployed through openings in the exo-skeleton when the robot is at rest, and retracted before it resumes motion. The camera can be used for reconnaissance but successful operation will require its point of deployment to be vertically upright whenever the robot comes to rest. This feature of the motion planner will also enable proper deployment and operation of manipulators and limbs. It is envisioned that Spherobots will be useful in different scenarios; these scenarios are not discussed here.

In our endeavour to making spherobots a reality, we address the motion planning problem. This problem is defined as the task of converging a sphere, rolling without slipping on a flat surface, from an initial configuration to a final configuration. The problem, referred to as the ball-plate problem, has been of particular interest to researchers since its kinematic model cannot be reduced to chained-form [9]; this renders regimented nonholonomic control techniques inapplicable [1]. However, it has been shown by Li and Canny [8] that the ball-plate system and even the ball-ball system is completely controllable. In their paper they also presented a three-step algorithm for reconfiguration of the two position and three orientation coordinates of a sphere rolling on a flat surface. The first step converges the position coordinates. The second step converges two of the three orientation coordinates using

0-7803-5250-5/99/$10.00 © 1999 IEEE

Lie Bracket motion. On the surface of the sphere, such motion generates a spherical triangle. The third step uses a circular trajectory to converge the last orientation coordinate. The ball-plate system was revisited in [1], [5]. A kinematic model with triangular structure was used in [1] to simplify integration of the state equations and arrive at a system of nonlinear equations that provide the solution to the appropriate control inputs. In own words of the authors [1], the planner requires excessive computational time and may possess abnormal extremals. An open loop strategy, optimal in the sense of control minimization, was presented by Jurdjevic [5]. The results are elegant but similar to [1], the computational efficiency limits usefulness of the algorithm for practical implementation.

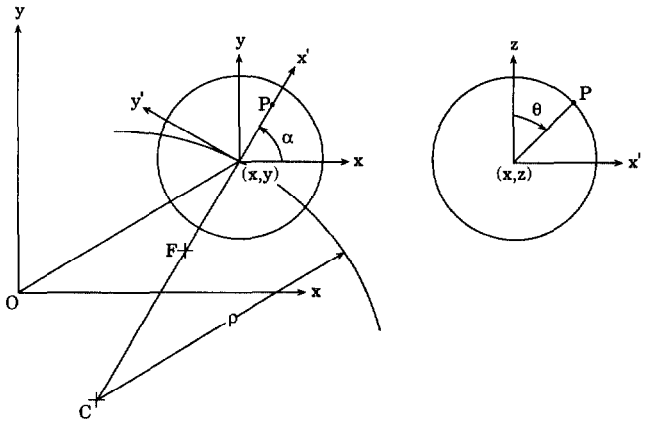

Figure 2. Description of state variables

The kinematic model of the sphere is discussed in section 2. The first strategy, based on spherical trigonometry, in presented in section 3. Though it bears resemblence to the second step of the algorithm in [8], it eliminates the third step of [8] using general spherical triangles, as opposed to equatorial spherical triangles. The second strategy, which uses a different kinematic model, is presented in section 4. Section 5 presents simulation results.

2 Kinematic Model

Consider the spherobot, shown in Fig.2. The Cartesian coordinates of the center of the robot are x, y, and P denotes the point of camera deployment. The diametrical plane x'-z, containing P, is inclined at angle α, $-\pi \leq \alpha \leq \pi$, with respect to the x-z plane. In this plane, P is located at angle θ, $0 \leq \theta \leq \pi$, relative to the top most point. The angular velocities of the robot about the x' and y' axes are ω'_x and ω'_y; these are also the control inputs. The robot configuration can be completely described by the four states x, y, θ, and α. Assuming unit radius of the sphere, the state equations can be written as follows

$$\dot{x} = \omega'_y \cos\alpha + \omega'_x \sin\alpha \quad (1)$$

$$\dot{y} = \omega'_y \sin\alpha - \omega'_x \cos\alpha \quad (2)$$

$$\dot{\theta} = \omega'_y \quad (3)$$

$$\dot{\alpha} = -\omega'_x \cot\theta \quad (4)$$

The above model does not completely describe the configuration of the sphere. Specifically, the model does not capture the orientation of the robot about the axis passing through point P and the center. However, it can still be used for partial or complete reconfiguration of the sphere. This will be shown in the next section.

3 Planning using Spherical Triangles

3.1 Sphere rolling along spherical triangle

Since a spherical triangle is a closed path on the surface of the sphere, the point of contact with the ground after rolling will be the same as the one before rolling. The sphere will however undergo a net rotation about the vertical axis passing through the contact point. Although the spherical triangle is a closed path on the sphere, it does not generate a closed path on the ground. In this section we obtain expressions for the net translation and rotation of the sphere in terms of the dimensions of the spherical triangle.

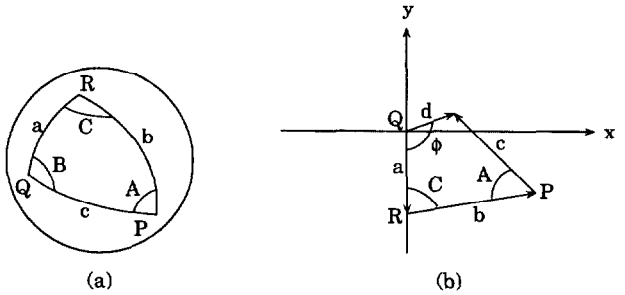

Figure 3. (a) A spherical triangle (b) Image of the spherical triangle on the x-y plane.

Let the center of the sphere initially be at the origin of the xyz coordinate frame, shown in Fig.3 (b). Let point Q in Fig.3 (a) be in contact with the ground. To roll along the spherical triangle PQR, the sphere is first rolled by the distance a in the negative y direction. This changes the contact point to R. The sphere is then rolled by distance b after a left turn of angle C with the previous direction. This brings the contact point to P. Finally, the sphere is rolled by distance c after a left turn of angle A. The sphere returns to its original contact point Q. In the x-y plane, the final position of the sphere center is denoted by the distance d and angle ϕ, measured with the initial direction of rolling, namely the negative y direction. Using basic trigonometry, it can be shown

$$d^2 = a^2 + b^2 + c^2 - 2ac\cos(A+C) - 2ab\cos C - 2ab\cos A \quad (5)$$

$$\phi = \arctan\left(\frac{b\sin C - c\sin(A+C)}{a - b\cos C + c\cos(A+C)}\right) \quad (6)$$

Let i, j, k denote unit vectors along coordinate axes fixed inertially, and let i', j', k' denote unit vectors along axes that are fixed to the sphere. Let us suppose that the unit vector triads are coincident at the initial time. Since rolling along the spherical triangle is equivalent to a pure rotation about the z axis, the rotation matrix will have the form

$$\begin{pmatrix} i \\ j \\ k \end{pmatrix} = \begin{pmatrix} \cos\alpha & \sin\alpha & 0 \\ -\sin\alpha & \cos\alpha & 0 \\ 0 & 0 & 1 \end{pmatrix} \begin{pmatrix} i' \\ j' \\ k' \end{pmatrix} \quad (7)$$

where α is the amount of rotation about the positive z axis. To obtain an expression for α we recall the general expression for rotation of r to r' about l by γ

$$r' = (1 - \cos\gamma)(l \cdot r)\, l + \cos\gamma\; r + \sin\gamma\; (l \times r) \quad (8)$$

Let i_1, j_1, k_1 denote unit vectors along the sphere fixed axes after the first roll about $l = i$ by angle $\gamma = a$. Then using Eq.(8), i_1, j_1, k_1 can expressed in terms of i, j, k, and a. The second roll is equivalent to a rotation about $l = [-\cos C\, i + \sin C\, j]$ by angle $\gamma = b$. Therefore, i_2, j_2, k_2, denoting sphere fixed unit vectors at the end of the second roll, can be expressed in terms of i_1, j_1, k_1, C, and b. The last rotation is about $l = [\cos(A + C)\, i - \sin(A + C)\, j]$ by angle $\gamma = c$. Therefore, i', j', k' can be obtained in terms of i_2, j_2, k_2, A, C, and c. Through substitution, the elements of the rotation matrix can be obtained in terms of sides and angles of the triangle PQR. After tedious simplification using spherical trigonometric identities [6] and several variants thereof, α can be expressed as [10]

$$\alpha = \pi - (A + B + C) \leq 0 \quad (9)$$

which is equivalent to the negative of the area of the spherical triangle. The path taken by the sphere in Fig.3 (b) can be considered as left-handed since left turns were taken at Q and R. It is straightforward to show for a right handed path, α would take the form

$$\alpha = (A + B + C) - \pi \geq 0 \quad (10)$$

which is equivalent to the area. In summary, when a sphere rolls along a sphericle triangle, the final location of the sphere can be computed using Eqs.(5), and (6); the net rotation about the vertical axis can be computed from Eq.(9) or (10), depending upon whether the path is left-handed or right-handed, respectively.

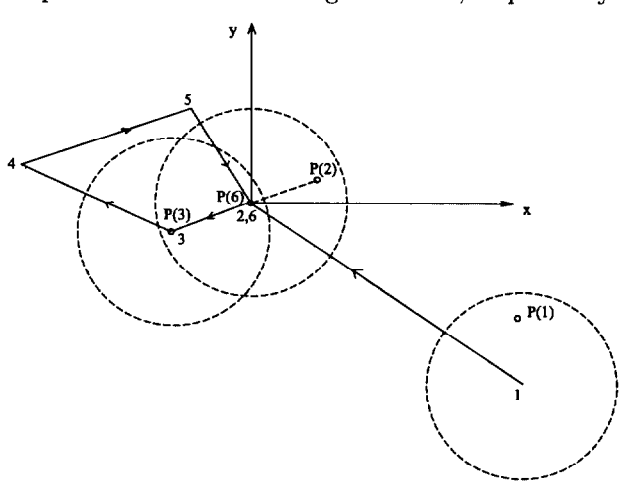

Figure 4. Motion planning using spherical triangles.

3.2 Formulation of open-loop strategy

In this section we formulate an open loop control strategy to reconfigure the sphere. In reference to Fig.4, this constitutes positioning the sphere at the origin of the x-y frame, locating point P at the top of the sphere, and providing an arbitrary orientation to the sphere with point P on top. At the initial configuration, marked 1 in Fig.4, point P is arbitrarily located at $P(1)$. Our strategy consists of three steps. First, the sphere rolls from the initial configuration to the origin of the x-y frame, denoted by the straight line path $1 \rightarrow 2$ in Fig.4. P is then located at an arbitrary point on the sphere, $P(2)$. Second, the sphere rolls away from the origin to bring point P to the top. This is shown by the straight line trajectory $2 \rightarrow 3$. Finally, a spherical triangular path is chosen to transfer the sphere back to the origin and simultaneously provide the proper amount of rotation. At the end of the path, P is guaranteed to return to the top. The path on the ground traced by the sphere is comprised of the segments $3 \rightarrow 4$, $4 \rightarrow 5$, and $5 \rightarrow 6$. The first two steps are trivial to implement. The last step requires us to find a spherical triangle whose sides and angles satisfy Eqs.(5), (6), and (9) or (10), for given d, ϕ, α.

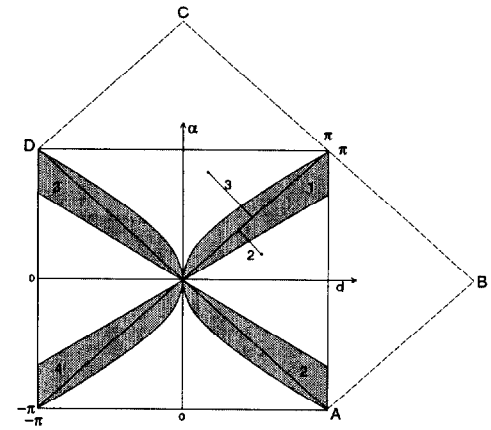

Figure 5. Reachable space in d-α.

Before we proceed with any computation, we investigate existence of a solution. First, since the second step of our algorithm involves a roll of no more than π, and the radius of the sphere is unity, we have $0 \leq d \leq \pi$. Next, since ϕ is measured from the direction in which the sphere begins to roll, which is arbitrary, values of ϕ differing by 180° can be achieved for the same value of d. Hence we can effectively expand the reachable space of d to $-\pi \leq d \leq \pi$. Finally, positive and negative values of α can be achieved with right- and left-handed paths. With these observations we plot in Fig.5 all values of d, α that can be achieved with $0 \leq a, b, C \leq \pi$. Of course, for every set of values of a, b, C, we first determine A, B, and c, using Eqs.(5). These values are substituted in Eqs.(5) and (9) to determine d and α. The grey area in Fig.5 indicates that all values of d, $0 \leq d \leq \pi$, and α, $-\pi \leq \alpha \leq \pi$, cannot be reached using one spherical trianglular path. However, we assert that it can be achieved with atmost two spherical triangular paths.

To prove our assertion, we consider the straight lines 1, 2, 3, 4 in Fig.5, which are conservative estimates of the reachable space of d-α. To prove our assertion, we translate lines 2 and 3 by moving their common point along line 1. This generates the rectangular parallelopiped $ABCD$ which contains the entire region $0 \leq d \leq \pi$, $-\pi \leq \alpha \leq \pi$. It can now be argued that any point in this region can be reached by first moving to a point on line 1, and then to a point which lies on a line that is parallel to line 2 or line 3 in Fig.5.

4 Simple Geometric Motion Planner

4.1 Two specific control actions

Consider the motion of the spherobot in Fig.2, whose kinematic model is given by Eqs.1-4, for the

two specific control actions:

(a) $\omega'_y \neq 0$, $\omega'_x = 0$

(b) $\omega'_x \neq 0$, $\omega'_y = 0$, $\theta \neq 0$

For action (a), the sphere moves along a straight line as θ changes. Let F be the fixed point on this straight line where the sphere would have $\theta = 0$. Since the sphere rolls without slipping, this point remains invariant. For action (b), the instantaneous radius of curvature of the path traced by the sphere on the x-y plane is obtained from Eqs.(1) and (2), and their derivatives

$$\rho = \frac{\left(\dot{x}^2 + \dot{y}^2\right)^{3/2}}{\dot{x}\,\ddot{y} - \dot{y}\,\ddot{x}} = \tan\theta \tag{11}$$

Since $\omega'_y = 0$, the sphere moves along a circular path; the center of this circle lies at C in Fig.2. For action (a), C moves away from F as θ increases, and converges to F as θ converges to zero.

4.2 Prelude to complete reconfiguration

In this section we present an algorithm to converge (x, y, θ, α) from $(x_0, y_0, \theta_0, \alpha_0)$ to $(0, 0, 0, \alpha_f)$. This strategy will be used to develop the complete reconfiguration algorithm, discussed in the next section. With reference to Fig.6, the algorithm can be stated as:

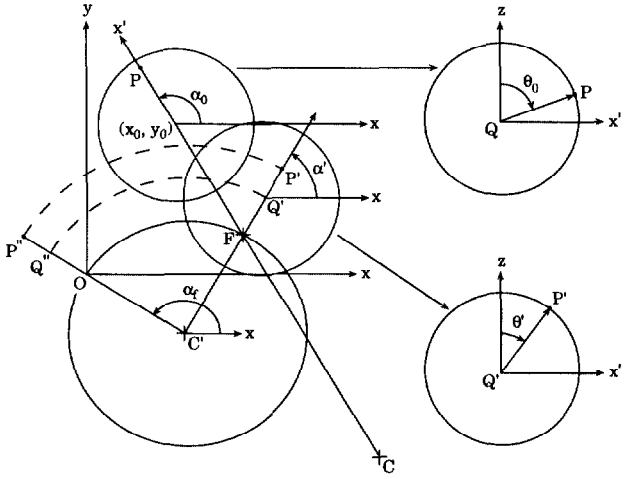

Figure 6. Basis for complete reconfiguration

1. Find the unique circle passing through O and F, whose center lies on the line that passes through the origin with slope α_f. Let C' be the center of this circle, and let α' be the slope of line $C'F$. Execute control action (a), wherein θ is changed from θ_0 to zero, to move C to F and P to the top most position. During this process, the center of the sphere moves from $Q = (x_0, y_0)$ to F.

2. Execute control action (a) to move the center of curvature of the sphere from F to C'. This will entail rolling the sphere in the direction α' by some distance θ'. During this process, the center of the sphere rolls from the fixed point F to Q', and P moves from the top to P'.

3. Execute control action (b) to bring F to the origin along the circle designed in the first step. This will move points P' and Q' to P'' and Q'', respectively. The trajectories of P', Q' will be concentric with that of F. During this motion, θ' does not change.

4. Execute control action (a) to bring the center of the sphere, Q'', to the origin. This will bring P'' to the top most position since O is the image of F with $\theta = 0$. This completes the reconfiguration.

To solve the problem mathematically, locate coordinates $C' \equiv (a, b)$. Since (a, b) lies on the straight line passing through the origin with slope α_f, we have

$$b = a \tan\alpha_f \tag{12}$$

Since the sphere has unit radius, the coordinates of point F are $F \equiv (x_0 - \theta_0 \cos\alpha_0, y_0 - \theta_0 \sin\alpha_0)$. Equating the distances OC' and FC' in Fig.6, we get

$$a^2 + b^2 = (a - x_0 + \theta_0 \cos\alpha_0)^2 + (b - y_0 + \theta_0 \sin\alpha_0)^2 \tag{13}$$

Using Eqs.(12) and (13), we solve for a as

$$a = \frac{x_0^2 + y_0^2 + \theta_0^2 - 2\theta_0(x_0 \cos\alpha_0 + y_0 \sin\alpha_0)}{2(x_0 + y_0 \tan\alpha_f - \theta_0(\cos\alpha_0 + \sin\alpha_0 \tan\alpha_f)} \tag{14}$$

Subsequently, b can be obtained using Eq.(12). The term $\tan\alpha_f$ in Eqs.(12) and (14) does not pose any problem since coordinate axes can be chosen such that $\alpha_f \neq 90°$. After a and b have been obtained, θ', $0 \leq \theta' \leq \pi/2$, can be solved from the relation

$$\tan\theta' - \theta' = \sqrt{a^2 + b^2} \tag{15}$$

The above equation is derived from the relations $OC' = FC'$, $FQ' = \theta'$ and $C'Q' = \tan\theta'$. Using coordinates of F and C', α' can be solved as follows

$$\tan\alpha' = \frac{(y_0 - \theta_0 \sin\alpha_0 - b)}{(x_0 - \theta_0 \cos\alpha_0 - a)} \tag{16}$$

4.3 Complete reconfiguration

Consider again the algorithm in section 4.2. The first step of the algorithm, step 1, is trivial and brings point P to the top. This configuration is shown again in Fig.7 for convenience. At this configuration, define point q to be any point on the equatorial circle. Without any loss of generality, it is taken to be the point on the x' axis. The complete reconfiguration problem may now be cast as the task of designing a path that brings the sphere to point O in Fig.6, point P back to the top, and provide a specified change in orientation of q. To address this problem we recant steps 2, 3, and 4 of the algorithm in section 4.2. These steps indeed bring the sphere center to point O and point P to the top. Our purpose is to compute the change in orientation of q on the equatorial plane.

Figure 7 captures the motion of the sphere as it repeats steps 2, 3, and 4 of the algorithm in section 4.2. It is, in essence, a three dimensional rendition of Fig.6. During step 2, under control action (a), as θ moves to θ', $P \rightarrow P'$, $Q \rightarrow Q'$ and $q \rightarrow q'$. Note that $P'Q'$ is still orthogonal to the equatorial circle containing q'. During step 3, under control action (b), θ is maintained at θ' while the sphere rolls along the circular path shown. A contact circle is formed on the surface of the sphere that is perpendicular to the $P'Q'$

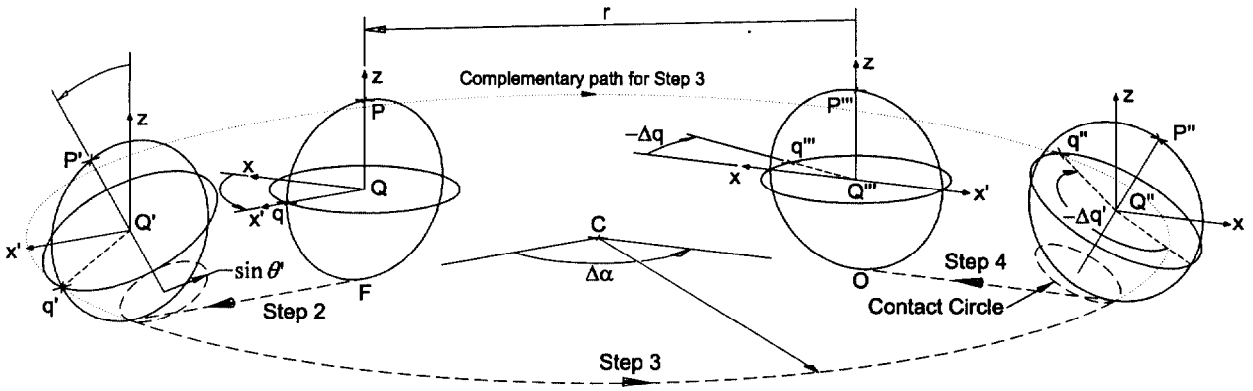

Figure 7. Complete reconfiguration strategy.

axis and has radius $\sin\theta'$. As $P' \rightarrow P''$ and $Q' \rightarrow Q''$, the $x'y'$ frame rotates relative to the fixed xy frame about axis z to produce a net change in α. This change, denoted by $\Delta\alpha$, can be expressed as $\Delta\alpha = \alpha_f - \alpha'$ in reference to Fig.6. Using Eq.(4), it can be written as

$$\Delta\alpha = -\cot\theta' \int \omega'_x dt \tag{17}$$

In effect, control action (b) in step 3 produces a pure rotation about the $P'Q'$ axis wherein the contact circle, shown in Fig.5, acts as an inclined disk rolling on the ground. The equitorial circle therefore maintains its orthogonality with $P'Q'$. During this process, the point q' rotates in the equitorial plane by an amount $\Delta q'$, which can be expressed as

$$\Delta q' = \frac{1}{\sin\theta'} \int \omega'_x dt \tag{18}$$

Using Eqs.(17) and (18), we get

$$\Delta q' = -\frac{1}{\cos\theta'} \Delta\alpha \tag{19}$$

For a positive change in angle α, as shown in Fig.7, the change in orientation of q' is negative. This is true since the equatorial circle rotates about the negative $P'Q'$ axis. During step 4, the use of control action (a) results in $\theta \rightarrow 0$ and $P'' \rightarrow P'''$, $Q'' \rightarrow Q'''$. Hence the inclined equatorial plane containing q'' returns to the xy plane. The angle of q''', relative to the fixed x-axis, Δq, is expressed as

$$\Delta q = \Delta\alpha + \Delta q' = \Delta\alpha(1 - 1/\cos\theta') \tag{20}$$

In the above expression, angle Δq is the net reorientation of point q in the equatorial plane. Though it is shown as a function of both $\Delta\alpha$ and θ', it is only a function of $\Delta\alpha$ since θ' is related to $\Delta\alpha$ by the relation

$$\tan\theta' - \theta' = \frac{r}{2\sin(\Delta\alpha/2)} \tag{21}$$

Clearly, Δq can be uniquely defined from $\Delta\alpha$, and vice versa. Naturally, the complete reconfiguration problem can be cast in the framework of the partial reconfiguration with the additional requirement of changing α by $\Delta\alpha$, that corresponds to the prescribed value of Δq. The algorithm for achieving this task was provided in the last section. In this section we now show that any $\Delta q \in [0, 2\pi]$ can be achieved through feasible changes in α, namely $\Delta\alpha$.

We first note that Eq.(21), which gives us the expression for $\Delta\alpha$ as a function of θ' can be written as

$$\Delta\alpha = 2\arcsin\frac{r}{2(\tan\theta' - \theta')} \tag{22}$$

To understand the limits of $\Delta\alpha$ consider the case where point C is at ∞. In such a case, $\Delta\alpha \rightarrow 0$ and the circular arc in step 3 tends to a straight line of infinite radius. This corresponds to $\theta' = \pi/2$, as seen from the expression of ρ in Eq.(11), and it leads to $\Delta\alpha = 0$. The other extreme case occurs when point C lies in the middle of the line joining points O and F. In this case, it is quite simple to show that $(\tan\theta' - \theta') = r/2$ and $\Delta\alpha = \pi$. Equation (22) holds true if the sphere travels along the circular path in Fig.7. If the sphere takes the complementary circular path, then the expression for $\Delta\alpha$ will be given by the relation

$$\Delta\alpha = -2\pi + 2\arcsin\frac{r}{2(\tan\theta' - \theta')} \tag{23}$$

From Eq.(23), the limits of $\Delta\alpha$ can be shown to be in the range -2π to $-\pi$, or 0 to $-\pi$. If we consider the fact that the sphere can take the direct path or the complementary path, the change in α can be chosen to lie in the range of $-\pi$ to π.

Using the limiting values of $\Delta\alpha$, it can be shown that $\pi(1 - 1/\cos\theta') \leq \Delta q \leq -r$ for the direct circular path, and $-\pi(1 - 1/\cos\theta') \leq \Delta q < \infty$ for the complementary circular path. These limits clearly indicate that any change of Δq in the range $[0, 2\pi]$ can be achieved.

To completely reconfigure the spherobot, we would first execute step 1 of the algorithm in section 3.3. At this point we will know the coordinates of r, $r \equiv (x_0 - \theta_0\cos\alpha_0, y_0 - \theta_0\sin\alpha_0)$, and Δq would be given to us. From the value of Δq, we will solve for θ' using Eq.(20) and one among Eqs.(22) and (23). Specifically, we will be using one of the following equations

$$\Delta q = 2\arcsin\frac{r}{2(\tan\theta' - \theta')}\left(1 - \frac{1}{\cos\theta'}\right)$$

$$\Delta q = -2\pi + 2\arcsin\frac{r}{2(\tan\theta' - \theta')}\left(1 - \frac{1}{\cos\theta'}\right)$$

After evaluating θ', $\Delta\alpha$ can be evaluated using Eq.(20). Subsequently, α_f and α' can be obtained using simple

trigonometry, from the following equations

$$\alpha_f = \arctan\left(\frac{y_0 - \theta_0 \sin\alpha_0}{x_0 - \theta_0 \cos\alpha_0}\right) + \frac{\pi}{2} + \frac{\Delta\alpha}{2} \quad (24)$$

$$\alpha' = \arctan\left(\frac{y_0 - \theta_0 \sin\alpha_0}{x_0 - \theta_0 \cos\alpha_0}\right) + \frac{\pi}{2} - \frac{\Delta\alpha}{2} \quad (25)$$

The coordinates of point C can be finally computed from Eqs.(12) and (14).

5 Simulation Results

Simulation results are presented for complete reconfiguration of the sphere. The initial coordinates of the sphere were assumed to be at $(x, y, \theta, \alpha) \equiv (4.33, 2.50, 30, 75)$. The desired final orientation was $\alpha_f = 180°$. In the first step, control action (a) first drives θ to zero, shown by trajectory a to b in Fig.8 (a). In the second step control action (a) changes θ to 75.6° in the direction of $\alpha' = 50.9°$. This is shown by the trajectory from b to c. In the third step control action (b) rolls the sphere along a circular path, keeping θ constant. At the end of this path the orientation of the sphere α reaches 180°, as desired, the center of the sphere reaches point d, and the fixed point F converges to the origin. Control action (a) is applied as the fourth and last step to bring θ to zero and the sphere to the origin, point e. The evolution of states x, y, are shown in Fig.8 (b); states θ, α are shown in Fig.8 (c).

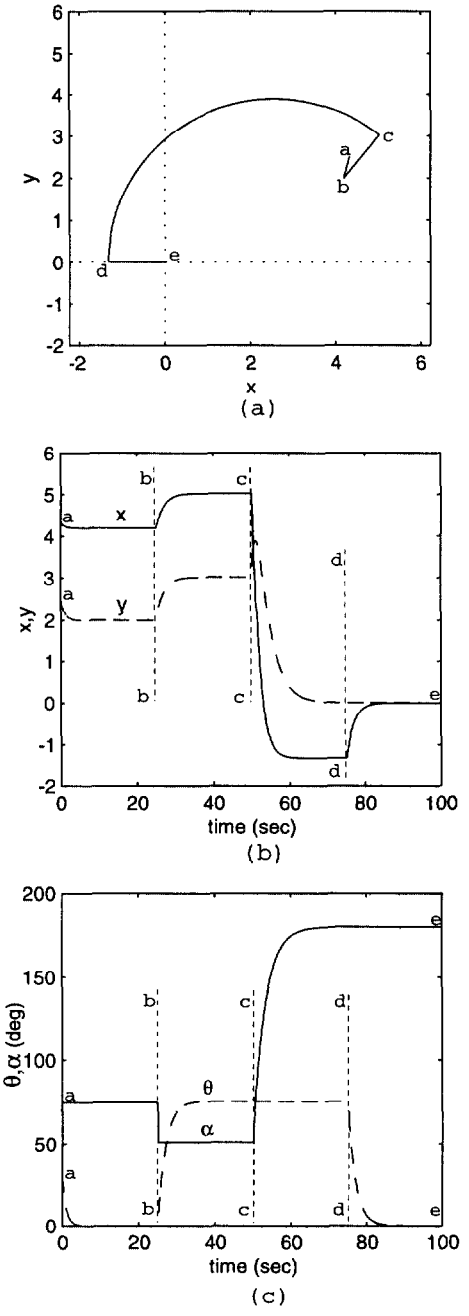

Figure 8. Evolution of state variables during complete reconfiguration.

6 Conclusion

A brief overview of the design of a spherical mobile robot was first presented. In light of the desired capabilities of the robot, the problem of reconfiguration of a sphere on a flat surface was addressed. Existing open loop strategies were discussed and our strategy was presented. Our strategy relies on a particular kinematic model of the sphere that results in linear and circular motions of the sphere on the plane for individual control inputs. Using individual inputs, two algorithms were presented for partial and complete reconfiguration. As compared to existing motion planners, most of which require intensive numerical computation, our reconfiguration strategies involve solving simple equations and provide the scope for easy implementation. Our future work is aimed at development of closed loop control strategies for reconfiguration.

Acknowledgement

The authors acknowledge the support provided by the National Science Foundation, Grant CMS-98000343.

References

[1] Bicchi, A., Prattichizzo, D., and Sastry, S. S., 1995, "Planning Motions of Rolling Surfaces", Proc. 34th Conference on Decision and Control, pp.2812-2817.

[2] Bicchi, A., Balluchi, A., Prattichizzo, D., and Gorelli, A., 1997, "Introducing the Sphericle: An Experimental Testbed for Research and Teaching in Nonholonomy", Proc. IEEE Int. Conference on Robotics and Automation, pp.2620-2625.

[3] Brown, H. B., and Xu, Y., 1997, "A Single-Wheel Gyroscopically Stabilized Robot", IEEE Robotics and Automation Magazine, Vol.4, No.3, pp.39-44.

[4] Halme, A., Schonberg, T., and Wang, Y., 1996, "Motion Control of a Spherical Mobile Robot", Proc. AMC'96-MIE.

[5] Jurdjevic, V., 1993, "The Geometry of the Plate-Ball Problem", Archives for Rational Mechanics and Analysis, 124, pp.305-328.

[6] Koshiyama, A., and Yamafuji, K., 1993, "Design and Control of All-Direction Steering type Mobile Robot", International Journal of Robotics Research, Vol.12, No.5, pp.411-419.

[7] Li, Z., and Canny, J., 1990, "Motion of Two Rigid Bodies with Rolling Constraint", IEEE Transactions on Robotics and Automation, Vol. 6, No. 1, pp.62-72.

[8] Murray, R. M., and Sastry, S. S., 1993, "Nonholonomic Motion Planning: Steering Using Sinusoids", IEEE Trans. on Auto. Cont., 38(5), pp.700-713.